Research, Society and Development, v. 10, n. 5, e56510515336, 2021
(CC BY 4.0) | ISSN 2525-3409 | DOI: http://dx.doi.org/10.33448/rsd-v10i5.15336

A 3D finite element analysis of bone tissue in three-unit implant-supported prostheses configurations through varying configuration factors (single-unit and splinted crowns in straight-line and offset configurations) and implant lengths in the maxillary posterior region

Análise tridimensional de elementos finitos do tecido ósseo em próteses sobre implante de três elementos variando a esplintagem, posicionamento e comprimento dos implantes em região posterior de maxilla

Análisis tridimensional de elementos finitos de tejido óseo en prótesis sobre implantes de tres unidades variando la ferulización, posicionamiento y longitud de los implantes en la región posterior del maxilar

Received: 04/22/2021 | Reviewed: 05/03/2021 | Accept: 05/04/2021 | Published: 05/16/2021

Victor Eduardo de Souza Batista
ORCID: https://orcid.org/0000-0003-0246-8101
University of Western São Paulo, Brazil
E-mail: victor_edsb@hotmail.com
Fellippo Ramos Verri
ORCID: https://orcid.org/0000-0001-5688-1669
Universidade Estadual de São Paulo, Brazil
E-mail: fellippo@gmail.com
Cleidiel Aparecido Araújo Lemos
ORCID: https://orcid.org/0000-0001-8273-489X
Federal University of Juiz de Fora, Brazil
E-mail: cleidiel@gmail.com
Ronaldo Silva Cruz
ORCID: https://orcid.org/0000-0003-3214-2479
Universidade Estadual de São Paulo, Brazil
E-mail: ronald.mb@hotmail.com
Pedro Yoshito Noritomi
ORCID: https://orcid.org/0000-0001-7333-3445
Universidade Estadual de São Paulo, Brazil
E-mail: pedro.noritomi@cti.gov.br
Eduardo Piza Pellizzer
ORCID: https://orcid.org/0000-0003-0670-5004
Universidade Estadual de São Paulo, Brazil
E-mail: ed.pl@uol.com.br

Abstract

The objective of the present study was to analyze the stress and microstrain on cortical bone tissue caused by occlusal forces on three-unit implant-supported prostheses placed in the maxillary posterior region through varying configuration factors and implant lengths using 3D finite element analysis. Fifteen three-dimensional models were simulated with the support of the In Vesalius, SolidWorks 2016, and Rhinoceros 4.0 software programs. Each three-dimensional model included a maxillary bone block corresponding to the region from the 1st premolar to the 1st right molar with three EH implants measuring 4.0 mm in diameter, which supported the three-unit metal-ceramic screw-retained prosthesis through varying configuration factors (single-unit and splinted crowns: straight-line and tripod design) and implant lengths (10, 8.5, and 7 mm × Ø4 mm). The FEMAP 11.4.2 program was used to generate the finite element models in the pre- and post-processing phases. Bone tissue was analyzed using Maximum Principal Stress (MPa) and Microstrain (με) maps. The highest stress/microstrain values were observed in oblique loading. In addition, splinting associated with the offset configuration generated improved biomechanical behavior. Furthermore, the association of short implants with longer implants did not exhibit any biomechanical benefits. Moreover, a reduced implant length (i.e., 7 mm) generated unfavorable biomechanical behavior. Splinting was effective in reducing the stress/microstrain on cortical bone tissue, especially when associated with the offset configuration of the

implants. Also, an increased implant length decreased the stress/microstrain in the bone tissue, and splinted short implants presented similar biomechanical behavior to short implants associated with longer implants.
Keywords: Biomechanical phenomena; Finite element analysis; Dental implant.

Resumo

O objetivo do presente estudo foi analisar a tensão e a microdeformação do tecido ósseo cortical geradas pelas forças oclusais sobre próteses de três elementos implantossuportadas, variando o fator união e comprimento dos implantes, instaladas na região posterior de maxila. Quinze modelos tridimensionais foram simulados com auxílio dos programas In Vesalius, SolidWorks 2016, Rhinoceros 4.0. Cada modelo tridimensional foi constituído de um bloco ósseo maxilar referente à região do 1º PM ao 1º M direito, apresentando três implantes do tipo hexágono externo (HE) de 4,0 mm de diâmetro, suportando prótese de três elementos metalocerâmica parafusada, variando o fator união (coroas unitárias e esplintadas: em linha reta e em posicionamento tripoidal), comprimento com implantes (10 mm, 8,5 mm e 7 mm de Ø4 mm). O programa FEMAP 11.4.2 foi utilizado para gerar os modelos de elementos finitos nas fases de pré- e pós-processamento. A análise do tecido ósseo foi feita utilizando os mapas de Tensão Máxima Principal (MPa) e Microdeformação (με). Os maiores valores de tensão/microdeformação foram observados no carregamento oblíquo. A esplintagem associada ao posicionamento tripoidal gerou melhor comportamento biomecânico. A associação de implantes curtos com implante de maior comprimento não demonstrou benefício biomecânico. A redução do comprimento do implante (7 mm) gerou um comportamento biomecânico desfavorável. A esplintagem foi efetiva na redução de tensão/microdeformação do tecido ósseo cortical, principalmente quando associada ao posicionamento tripoidal dos implantes. O aumento do comprimento do implante diminuiu a tensão/microdeformação no tecido ósseo. Implantes curtos esplintados mostraram comportamento biomecânico similar a implantes curtos associados a implantes de maior comprimento.
Palavras-chave: Fenômenos biomecânicos; Análise de elementos finitos; Implantação dentária endo-óssea.

Resumen

El objetivo del presente estudio fue analizar la tensión y microdeformación del tejido óseo cortical generada por las fuerzas oclusales sobre las prótesis de tres elementos implantosoportados, variando la unión y longitud de los implantes, instalados en la región posterior del maxilar. Quince modelos tridimensionales se simularon y cada modelo tridimensional consistió en un bloque óseo maxilar referido a la región de la 1ª PM a la 1ª M derecha, presentando tres implantes de hexágono externo (HE) de 4.0 mm de diámetro, soportando una prótesis metalocerámica atornillada, variando el factor unión (coronas unitarias y ferulizadas: rectas y en posición tripoide), longitud con implantes (10 mm, 8,5 mm y 7 mm Ø4 mm). El análisis del tejido óseo se realizó utilizando los mapas de Máxima Máxima Tensión (MPa) y Microdeformación (με). Los mayores valores de la tensión/microdeformación se observaron en la carga oblicua. El entablillado asociado al posicionamiento del trípode generó un mejor comportamiento biomecánico. La asociación de implantes cortos con implantes más largos no ha demostrado un beneficio biomecánico. La reducción de la longitud del implante (7 mm) generó un comportamiento biomecánico desfavorable. La ferulización fue eficaz para reducir la tensión/microdeformación del tejido óseo cortical, especialmente cuando se asocia con el posicionamiento trípode de los implantes. El aumento de la longitud del implante disminuyó la tensión/microdeformación en el tejido óseo. Los implantes ferulizados cortos mostraron un comportamiento biomecánico similar al de los implantes cortos asociados con implantes más largos.
Palabras clave: Fenómenos biomecánicos; Análisis de elementos finitos; Implantación dental endoósea.

1. Introduction

The advent of dental implants has enabled the rehabilitation of patients with partial edentulism in a more functional way (Vogel et al., 2013). Nevertheless, the inadequate designs of implant-supported restorations can generate mechanical and biological complications, leading to the failure of both the dental implant and the prosthesis over the implant (Abu-Hammad et al., 2007, Verri et al., 2014). Clinical situations where the patient does not have the first premolars and molars, or the second premolars and molars are common, and so different forms of restoration can be projected. Thus, dental implants can be placed in a straight-line or offset configuration, and either single-unit or splinted crowns (metal-ceramic or metal-free) can be applied in the prosthetic phase (Weinberg, Kruger, 1996; Lemos et al., 2018).

The potential advantages of the offset configuration for implants (i.e., slight positioning in the vestibular or lingual surface of the central implant) have been studied since it was initially proposed (Weinberg, Kruger, 1996; Abreu et al., 2012; Batista et al., 2015; de Souza Batista et al., 2017). A systematic review published in 2015 did not report a consensus on the benefits of offset configurations. However, no in vitro studies within this systematic review simulated their biomechanical

behavior in the maxillary posterior region (Batista et al., 2015). Through 3D finite element methodology, a prior study on the biomechanical behavior of offset configurations in implants in the maxillary posterior region concluded that the offset configuration could reduce both stress and microstrain in cortical bone tissue. However, only Ø4×10 mm external hexagon implants were evaluated (de Souza Batista et al., 2017).

In this context, opting between splinting the prostheses over implants or not is a relevant question for clinical practitioners. On the one hand, some authors advocate that splinting enables stress distribution among the implants (Grossmann et al., 2005), mainly in designs based on the use of short implants or the association of short implants to a longer implant (Pellizzer et al., 2014; Pellizzer et al., 2015). This could reduce stress on the retaining screw and on the cortical bone tissue. On the other hand, single-unit crowns facilitate hygiene and provide better passivity of the crown, in addition to an enhanced emergence profile and gingival contour (Solnit, Schneider, 1998; Vázquez Álvarez et al., 2015). Regardless, with respect to generating improved biomechanical behavior in prosthetic structures and bone tissue, any advantages in splinting the prosthesis are still not well established, as there is no consensus in the literature on this subject.

In some clinical situations, maxillary sinus anatomy permits the utilization of longer implants in the premolar region. To rehabilitate such cases, the literature suggests that splinting short implants to a longer implant reduces the biomechanical risk (Pellizzer et al., 2014; Pellizzer et al., 2015). Nonetheless, Yang et al. observed a similar biomechanical performance between the splinting of short implants and the splinting of short implants with a long implant (Yang et al., 2014), which shows that there is controversy on this topic.

Finite element analysis is a methodology used to simulate situations that are difficult to reproduce in a clinical study. Thus, the possibility to predict biomechanically unfavorable situations by evaluating the amount of stress and/or microstrain on bone tissue using mathematical calculations allows the methodology to be applied in the field of implantology (Torcato et al., 2014; Verri et al., 2016; Verri et al., 2017).

Thus, the aim of the present study was to assess the stress and microstrain in cortical bone tissue caused by occlusal forces on three-unit implant-supported prostheses placed in the maxillary posterior region through varying configuration factors (single-unit and splinted crowns: straight-line and offset configurations) and implant lengths (10, 8.5, and 7 mm × Ø4 mm) using the 3D finite element analysis. The null hypothesis was that the variables in question would not affect the biomechanical behavior of cortical bone tissue.

2. Methodology

Experimental design

The methodology used in the present study to assess the stress and strain was the 3D-finite element analysis. The methodology followed previously published studies (Lemos et al., 2018; de Souza Batista et al., 2017). However, in the present study, the following variables were considered: Configuration factors (single-unit and splinted crowns in straight-line and offset configuration), implant lengths (10, 8.5, and 7 mm), and loading (axial and oblique).

Three-dimensional modeling

To represent the different clinical situations, fifteen 3D models were simulated (Table 1). Each 3D model consisted of a maxillary bone block corresponding to the region from the 1st premolar to the 1st right molar with three external hexagon (EH) implants measuring 4.0 mm in diameter (Conexão Sistemas de Prótesis Ltda.), which supported a three-unit metal-ceramic screw-retained prosthesis.

Table 1. Description of the simulated models.

Model	Characteristic	Length			Nº. of Nodes/ Elements
		1º PM	2º PM	1º M	
M1	Three-unit prostheses, straight-line	10 mm	10 mm	10 mm	742 713/ 1 631 660
M2	Splinted prothesis, straight-line	10 mm	10 mm	10 mm	720 243/ 1 593 455
M3	Splinted prothesis, offset configuration	10 mm	10 mm	10 mm	783 087/ 1 684 904
M4	Three-unit prostheses, straight-line	8.5 mm	8.5 mm	8.5 mm	848 648/ 1 787 598
M5	Splinted prothesis, straight-line	8.5 mm	8.5 mm	8.5 mm	789 989/ 1 694 719
M6	Splinted prothesis, offset configuration	8.5 mm	8.5 mm	8.5 mm	698 941/ 1 558 264
M7	Three-unit prostheses, straight-line	7 mm	7 mm	7 mm	786 169/ 1 694 060
M8	Splinted prothesis, straight-line	7 mm	7 mm	7 mm	725 861/ 1 598 665
M9	Splinted prothesis, offset configuration	7 mm	7 mm	7 mm	709 340/ 1 573 501
M10	Three-unit prostheses, straight-line	10 mm	8.5 mm	8.5 mm	833 345/ 1 764 983
M11	Splinted prothesis, straight-line	10 mm	8.5 mm	8.5 mm	773 212/ 1 669 827
M12	Splinted prothesis, offset configuration	10 mm	8.5 mm	8.5 mm	741 266/ 1 623 719
M13	Three-unit prostheses, straight-line	10 mm	7 mm	7 mm	819 762/ 1 743 659
M14	Splinted prothesis, straight-line	10 mm	7 mm	7 mm	754 523/ 1 640 937
M15	Splinted prothesis, offset configuration	10 mm	7 mm	7 mm	682 310/ 1 532 596

1º PM, first premolar; 2º PM, second premolar; 1º M, first molar; mm, millimeter. Source: Authors.

The bone block design was composed of trabecular bone in the central region, surrounded by 1 mm of cortical bone, simulating type IV bone (Lekholom, Zarb, 1985). Bone tissue was obtained from a CT scan in the In Vesalius software (CTI). The surfaces were then simplified using the Rhinoceros 4.0 software (NURBS Modeling for Windows).

The implant design was obtained by simplifying an original design of an EH implant measuring 4.0 mm in diameter (Verri et al., 2016). The positioning of the implant in the straight-line models was simulated with a distance of 7 mm, measured from center to center between the premolars, and a distance of 8.75 mm, also measured from center to center between the 2nd premolar and the 1st molar (Puri et al., 2007). In the models simulating the offset configuration, the central implant, corresponding to the 2nd premolar, was displaced 1.5 mm toward the vestibular direction (de Souza Batista et al., 2017; Puri et

al., 2007; Nishioka et al., 2011; Nishioka et al., 2009; Sütpideler et al., 2014). Furthermore, the simulated UCLA (Universal Castable Long Abutment) prosthetic abutment was the same for all situations, but with a rotational system for splinted prostheses and an anti-rotational system for single-unit prostheses. The crown height and occlusal table size of the screw-retained metal-ceramic prostheses were equal for all simulated models.

Accordingly, the implants, abutments, metal-ceramic crowns, and screws were simplified using the SolidWorks 2016 (SolidWorks Body) and Rhinoceros 4.0 software programs and were equal for the fifteen different models. Finally, all geometries were exported for discretization using FEMAP 11.4.2 finite element software (Siemens PLM Software Inc.).

Configuration of three-dimensional analysis

FEMAP 11.4.2 software was employed to generate the finite element models in the pre- and post-processing phases. In the pre-processing phase, the meshes were generated with solid parabolic tetrahedral elements. Moreover, the mechanical properties of each simulated material were assigned to the meshes by applying the values from the literature (Table 2) (Sertgöz, 1997; Savimay et al., 2005; Verri et al., 2017; Verri et al., 2017b). All materials were considered as homogeneous, isotropic, and linearly elastic. The total number of elements and nodes of the models are presented in Table 1. In the post-processing phase, the maps obtained through mathematical calculations in the NEi Nastran 11.1 program (Noran Engineering, Inc.) were read and plotted (see Finite Element Analysis section).

Table 2. Mechanical properties applied in finite element analysis.

Structure	Elastic modulus (E) (GPa)	Poisson ratio (ν)	Reference
Trabecular bone with low density (type IV bone)	1.10	0.30	Sevimay et al.[24] 2005
Cortical bone	13.7	0.30	Sertgöz[23] 1997
Titanium (abutment screw and dental implant)	110.0	0.35	Sertgöz[23] 1997
Ni-Cr alloy	206.0	0.33	Verri et al.[25] 2017
Feldspathic porcelain	82.8	0.35	Verri et al. [25] 2017b

Source: Authors.

Contact, contour, and loading conditions

The contact conditions were also defined in the pre-processing phase, with juxtaposed contact only in the contact interface between the prosthetic component and implant, while bonding took place between the other contact interfaces. The contour conditions were fixed in all axes (x, y, and z), simulating fixation of the maxilla to the viscerocranium. Thus, following application of the loads, the overall crown/components/implant structure and all bone tissue surrounding the implants could move and undergo intrusion, leaving only the base of the bone block fixed in place and immobile (de Souza Batista et al., 2017). A force of 400 N was applied in the axial direction, with 50 N in the middle of the transverse edge of each canine tooth. In addition, 200 N of oblique force was applied, with 50 N at 45º in the middle of the transverse edge of each vestibular canine tooth.

Finite element analysis

All analyses were processed using Nei Nastran software version 11.1. The processing analysis of the models was performed at an HP workstation (Hewlett-Packard Development Company). Following data processing, the results were

transferred to FEMAP 11.4.2 to graphically view the stress/microstrain in the bone tissue through Maximum Principal Stress and Microstrain maps. The Maximum Principal Stress maps were used as criteria to analyze stress in the bone tissue, since they can provide values of compression (negative values) and tension (positive values) (Verri et al., 2014; Lemos et al., 2018; de Souza Batista et al., 2017; Torcato et al., 2014; Pellizzer et al., 2018). The microstrain analysis (με - strain ×10−6) criteria was also used to evaluate the bone tissue (de Souza Batista et al., 2017b) to acquire values for comparison with the resorption risk scale furnished by Frost (Frost, 2003). The unit of measurement used to measure the Maximum Principal Stress was MegaPascal (MPa). Microstrain (με) was measured by the strain unit ×10−6, and its magnitude is dimensionless.

3. Results

Maximum principal stress analysis

By assessing axial loading on a scale from - 5 to 10 MPa, low values of tension and compression were observed surrounding the implants for all proposed designs. In general, lower tensile and compressive values were observed in axial loading, while higher values were observed in oblique loading, especially in the case of tensile stress (Figures 1).

On a scale from - 10 to 40 MPa, the highest values of tensile stress occurred in the bone tissue of the palatine region around the implants, mainly around the 1st molar implant. Additionally, oblique loading generated a higher area of tensile stress in the palatine region of the 1st molar in the single-crown models (i.e., M1, M4, M7, M10, and M13), when compared to the splinted crowns. Among the splinted models, the clinical situations with straight-line implants (i.e., M2, M5, M8, M11, and M14) generated greater areas of tensile stress (15–36.8 MPa) in the bone tissue in the palatine region around the 2nd premolar when compared to implants with offset configurations (i.e., M3, M6, M9, M12, and M15). The offset configuration of the implants reduced the area of tensile stress in the palatine region of the bone tissue around the 1st molar of models M9, M12, and M15 compared to the values obtained for the corresponding straight-line splinted models M8, M11, and M14, respectively.

For designs with single-unit crowns, a reduced implant length generated a greater area of tensile stress on the bone tissue in the palatine region of the 1st molar, mainly for models M7 and M13. For models with straight-line splinted crowns, reducing the implant length from 10 to 8.5 mm (i.e., M2 to M5) did not generate unfavorable biomechanical behavior. However, a greater area of tensile stress on the bone tissue of the palatine region of the 1st molar in M8 was observed when compared to the same areas in models M2 and M5. For the models with splinted crowns in the offset configuration, model M3 exhibited the lowest tensile values, and a reduced implant length increased the area of tension in the bone tissue around the 1st premolar of models M6 and M9.

Figure 1. Maximum Principal Stress map. A, Cortical bone tissue. Axial loading, occlusal view. B, Cortical bone tissue. Oblique loading, occlusal view.

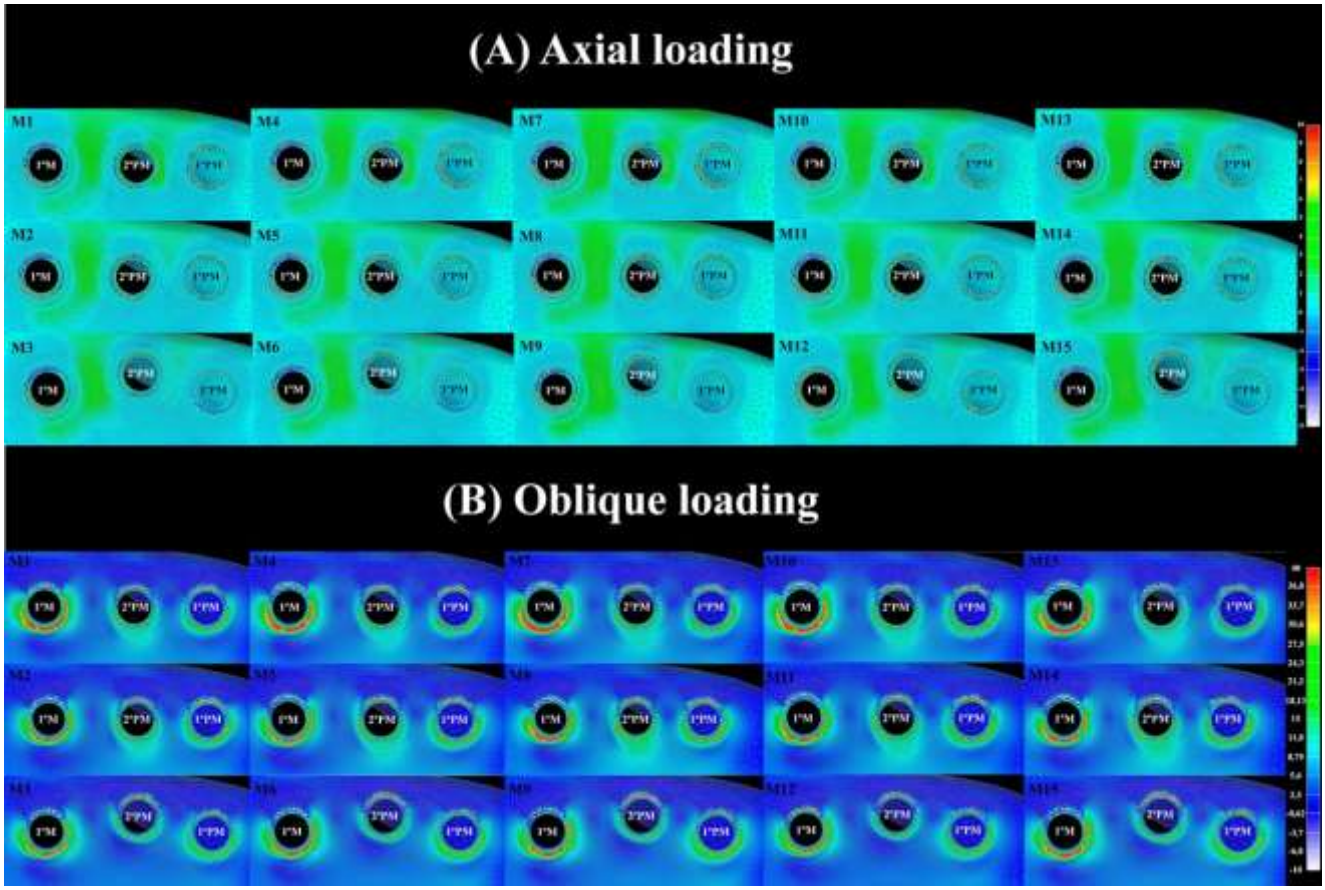

Source: Authors.

The association of short implants with longer implants in splinted crown designs demonstrated similar biomechanical behavior when compared to short implants, except in the comparison between M6 and M12, and especially for the 1st premolar region (Figure 2). The association of short implants with longer implants did not demonstrate biomechanical benefits for single-unit crowns.

Microstrain analysis

Under axial loading, on a scale from 0 to 3,000 με, the largest area of microstrain was found around bone tissue in the 1st molar region for all models. Generally, the lowest microstrain values were observed in axial loading, while the highest values were observed in oblique loading (Figure 3).

On a scale from 0 to 6000 με, the largest areas of microstrain occurred in the bone tissue of the vestibular region around the implants, mainly around the 1st molar implant. Clinical situations based on rehabilitation with single-unit implants (i.e., M1, M4, M7, M10, and M13) presented the largest areas of microstrain in the bone tissue of the vestibular area around the 1st molar when compared to rehabilitation with splinted implants. For the models with single-unit crowns (i.e., M1, M4, M7, M10, M13), reducing the implant length to 7 mm (M7) generated a larger area of microstrain in the bone tissue around the 1st molar implant, and the association of short implants with long implants did not demonstrate any biomechanical benefits (M10 and M13). Among the models with splinted crowns (i.e., M2, M3, M5, M6, M8, M9, M11, M12, M14, and M15), the straight-line implants (i.e., M2, M5, M8, M11, and M14) exhibited a larger area of microstrain in the bone tissue of the vestibular area around the 1st premolar and 1st molar when compared to implants in the offset configuration (i.e., M3, M6,

M9, M12, and M15). Nevertheless, implants in the offset configuration generated a greater area of microstrain in the bone tissue of the vestibular region of the 2nd premolar. Thus, splinted crowns with implants in the offset configuration exhibited enhanced biomechanical behavior compared to straight-line implants.

In addition, a decreased implant length was found to increase microstrain values, mainly in the bone tissue around the 1st molar implant for models with splinted crowns in the straight-line configuration and for implants in the offset configuration (Figure 4).

The association of short implants with longer implants in splinted crown designs resulted in similar biomechanical behavior when compared to clinical situations simulating all short implants.

Figure 2. Maximum Principal Stress values in cortical bone tissue under oblique loading. Blue, models with single-unit crowns; green, models with splinted crowns in the straight-line configuration; red, models with splinted crowns in the offset configuration.

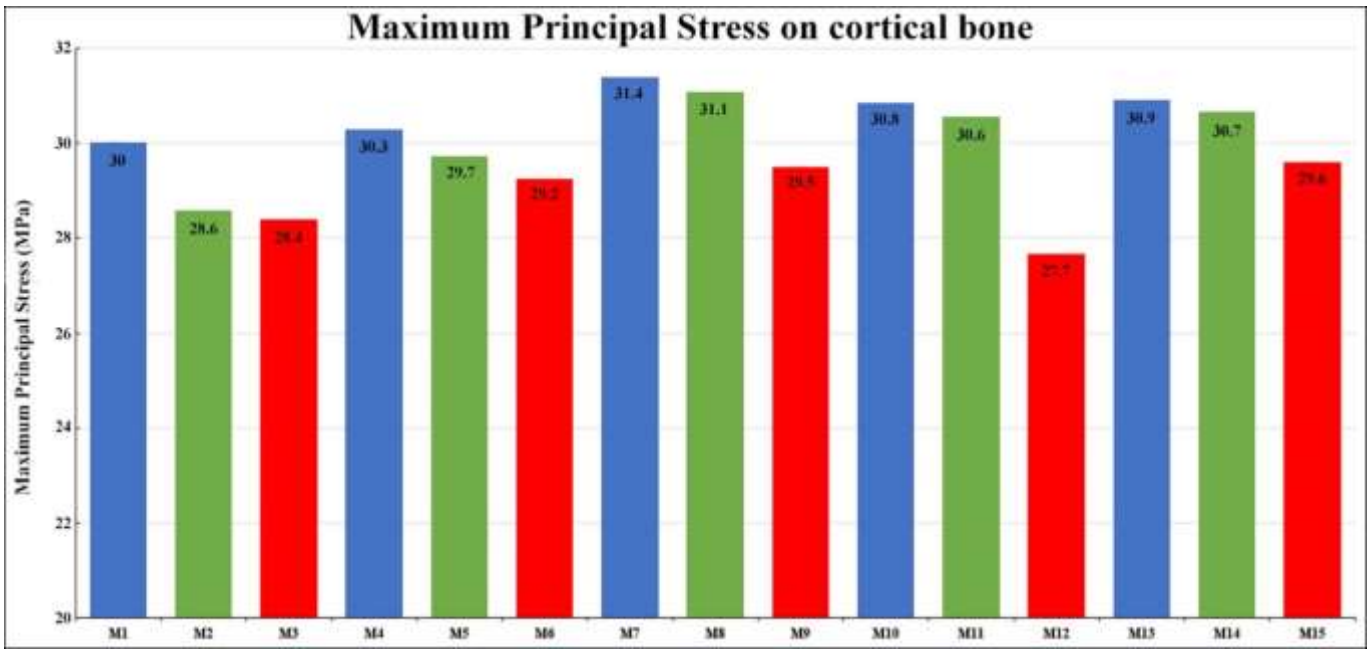

Source: Authors.

Figure 3. Maximum Principal Stress map. A, Cortical bone tissue. Axial loading, occlusal view. B, Cortical bone tissue. Oblique loading, occlusal view.

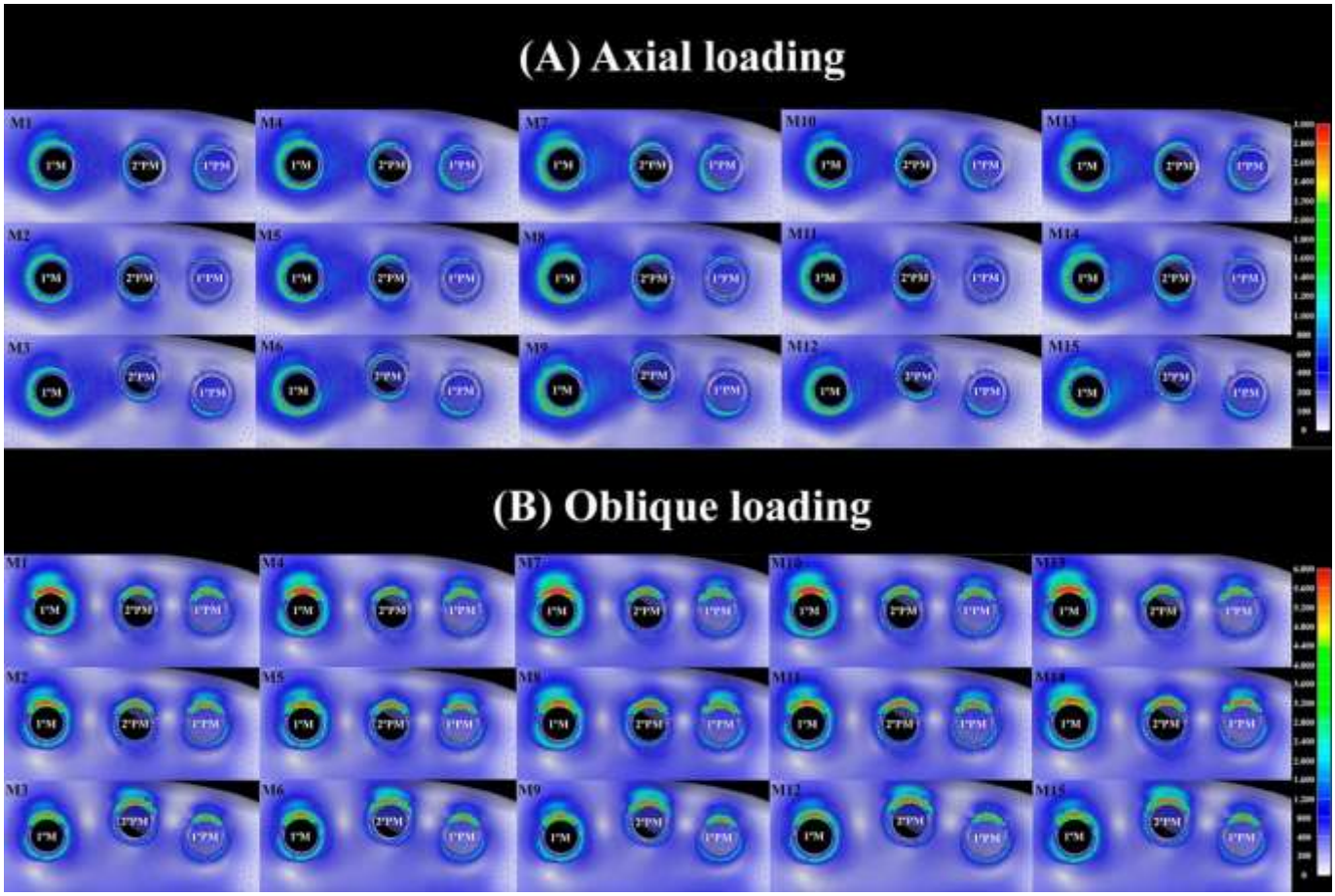

Source: Authors.

Figure 4. Microstrain values in cortical bone tissue under oblique loading.

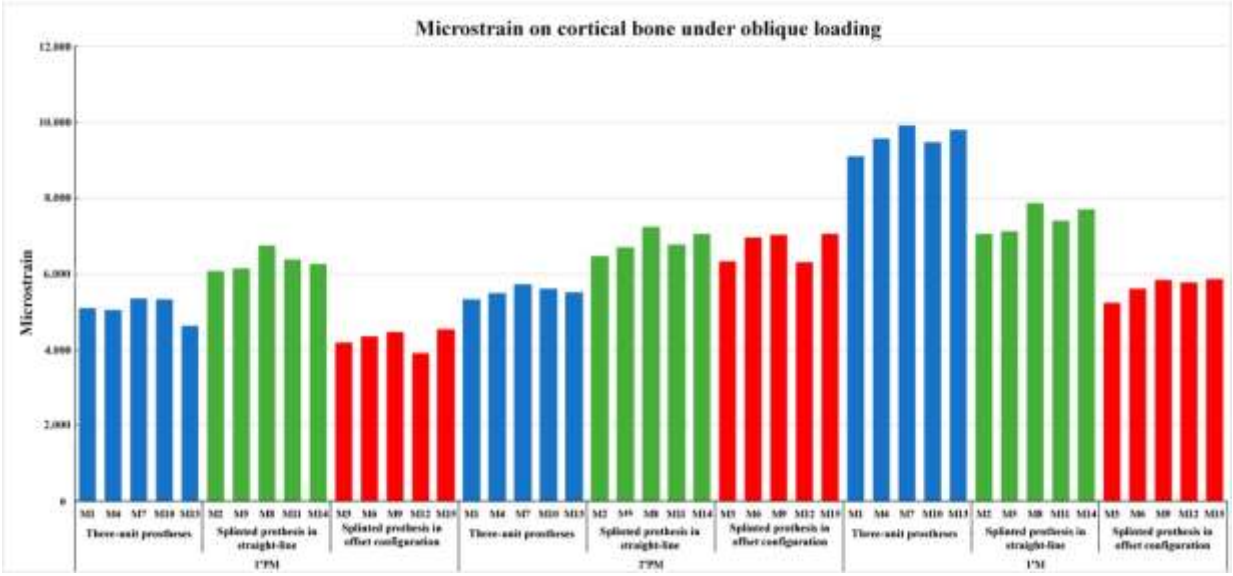

Source: Authors.

4. Discussion

The variables examined in this study, such as the splinting and implant configurations and changes in the implant lengths, resulted in different stress/strain distribution patterns in the bone tissue. Consequently, the null hypothesis of the present study was rejected.

The results obtained herein therefore suggested that splinting was effective in reducing the bone tissue stress/microstrain in designs with EH implants, especially when associated with the offset configuration of the implants. Indeed, these data corroborate previously published studies (de Souza Batista et al., 2017; Pellizzer et al., 2014; Sütpideler et al., 2004; Mendonça et al., 2014). For example, in 2014, Mendonça (Mendonça et al., 2014) suggested that rehabilitation with single-unit crowns in the posterior region may be more susceptible to masticatory forces, thereby increasing the risk of micromovement over the physiological limit. In the present study, the greatest degree of stress/microstrain was found in the bone tissue around the implant of the 1st molar region in restorations with single-unit crowns. This implant received the highest load quantity, according to the proposed methodology (200 N axial and 100 N oblique). Restorations with splinted crowns were effective in providing stress/microstrain distribution, especially when all implant lengths were reduced, thereby corroborating previously published studies that employed EH implants (de Souza Batista et al., 2017; Pellizzer et al., 2015). Thus, exercising caution in clinical routine, the splinting of EH implants positioned in the maxillary posterior region is suggested (de Souza Batista et al., 2017).

It was also found that adopting a standard implant length generated more favorable biomechanical behavior for strain/strain distribution in the bone tissue, thereby verifying the results of previous studies (Baggi et al., 2008; Ueda et al., 2017). As such, designs considering the use of EH implants in the maxillary posterior region should consider the length factor, since the utilization of longer implants may offer an enhanced biomechanical performance.

Previously published studies emphasized the benefit of associating short implants with longer implants, especially for implants smaller than 10 mm (Pellizzer et al., 2014; Pellizzer et al., 2015). Although this biomechanical advantage was not observed in the present study upon comparison among the splinted models, the association of short implants with longer implants resulted in lower stress/strain values compared to those obtained for single-unit implants. This allowed us to conclude that the benefits obtained from splinting predominated over the effect of implant length in designs based on EH implants.

The thresholds for a possible occurrence of bone tissue microdamage, as proposed by Frost, (Frost, 2003) are 60 MPa and 3000 με for the stress and the strain, respectively. Accordingly, the stress/microstrain values in cortical bone tissue that were collected from axial loading are within the proposed limit. In contrast, the stress/microstrain values in cortical bone tissue in oblique loading exceeded the proposed limit. Based on these results, it is necessary to highlight that the simulated bone tissue employed herein was considered to be isotropic, homogeneous, and linearly elastic, which may have contributed to such elevated values.

An improvement in the biomechanical behavior of bone tissue was observed upon the use of splinted implants in an offset configuration, thereby substantiating previously published studies (Batista et al., 2015; de Souza Batista et al., 2017). In addition, the application of oblique force in the internal region of the vestibular cusp generates a bending moment, which tends to overload the cervical region around the implants. However, the slight displacement to the vestibule of the central implant in splinted restorations possibly reduced the bending moment of the restoration, thereby decreasing stress/microstrain around the implants.

To date, few studies have evaluated the biomechanical behavior of offset configurations in the maxillary posterior region. Therefore, this study may contribute to an improved understanding of clinical situations where there is a requirement to work with EH implants with reduced lengths. However, the present study evaluated only one type of implant connection (i.e., EH). As the type of implant connection can influence the biomechanical behavior of the restoration (Goiato et al., 2015;

Minatal et al., 2017; Pellizzer et al., 2018), future biomechanical studies are required to examine the effect of implant length reduction, splinting, and its association with offset configurations in implants with internal connections (i.e., internal hexagon and Morse taper).

As restorations in the maxillary posterior region are difficult since it is an area that sustains more masticatory force in comparison to the anterior region (Itoh et al., 2004), clinical procedures such as adequate occlusal adjustment and reduction of the occlusal table are suggested to reduce stress/microstrain in the bone support tissue (Torcato et al., 2014).

5. Conclusion

Within the limitations of the study, it was possible to make a number of conclusions. Firstly, splinting was effective in reducing the stress/microstrain on cortical bone tissue, mainly in association with the offset configuration of the implants. In addition, an increased implant length decreased the stress/microstrain in bone tissue. Furthermore, splinted short implants exhibited a similar biomechanical behavior to short implants associated with longer implants. Indeed, these results are expected to improve the understanding of clinical situations where there is a requirement to work with external hexagon implants with reduced lengths.

Future biomechanical studies about the effects of implant length reduction, splinting, and its association with offset configurations in implants with internal connections.

Acknowledgments

The authors thank Renato Archer Research Center for their supporting in the analysis.

This research was supported by Scholarship of Research Foundation of the State of São Paulo – FAPESP # 2015/07383-8.

References

Vogel, R., Smith-Palmer, J., & Valentine, W. (2013). Evaluating the health economic implications and cost-effectiveness of dental implants: a literature review. *Int J Oral Maxillofac Implants*, 28, 343-356.

Abu-Hammad, O., Khraisat, A., Dar-Odeh, N., Jagger, D. C., & Hammerle, C. H. (2007). The staggered installation of dental implants and its effect on bone stresses. *Clin Implant Dent Relat Res*, 9, 121-127.

Verri, F. R., Batista, V. E., Santiago, J. F. Jr., Almeida, D. A., & Pellizzer, E. P. (2014). Effect of crown-to-implant ratio on peri-implant stress: a finite element analysis. *Mater Sci Eng C Mater Biol Appl*, 45, 234-240.

Weinberg L A, & & Kruger B. (1996). An evaluation of torque (moment) on implant/prosthesis with staggered buccal and lingual offset. *Int J Periodontics Restorative Dent*, 16, 252-265.

Lemos, C. A. A., Verri, F. R., Santiago, J. F. Jr., Almeida, D. A. F., Batista, V. E. S., Noritomi, P. Y., & Pellizzer, E. P. (2018). Retention system and splinting on morse taper implants in the posterior maxilla by 3D finite element analysis. *Braz Dent J*, 29, 30-35.

Abreu, C. W., Nishioka, R. S., Balducci, I., & Consani, R. L. X. (2012) Straight and offset implant placement under axial and nonaxial loads in implant-supported prostheses: strain gauge analysis. *J Prosthodont*, 21, 535-539.

Batista, V. E. S., Santiago, J. F. Jr., Almeida, D. A., Lopes, L. F., Verri, F. R., & Pellizzer, E. P. (2015). The effect of offset implant configuration on bone stress distribution: a systematic review. *J Prosthodont*, 24, 93-99.

de Souza Batista, V. E., Verri, F. R., Almeida, D. A. F., Santiago Junior, J. F., Lemos, C. A. A., & Pellizzer, E. P. (2017) Evaluation of the effect of an offset implant configuration in the posterior maxilla with external hexagon implant platform: A 3-dimensional finite element analysis. *J Prosthet Dent*, 118, 363-371.

Grossmann, Y., Finger, I. M., & Block, M. S. (2005). Indications for splinting implant restorations. *J Oral Maxillofac Surg*, 63, 1642-1652.

Pellizzer, E. P., Santiago, J. F. Jr., Ribeiro Villa, L. M., de Souza Batista, V. E., Mello, C. C., de Faria Almeida, D. A., & Honório H. M. (2014) Photoelastic stress analysis of splinted and unitary implant-supported prostheses. *Appl Phys B*, 117, 235-244.

Pellizzer, E. P., de Mello, C. C., Santiago, J. F. Jr., de Souza Batista, V. E., de Faria Almeida, D. A., & Verri, F. R. (2015). Analysis of the biomechanical behavior of short implants*: The photo-elasticity method. Mater Sci Eng C Mater Biol Appl*, 55, 187-192.

Solnit, G. S., & Schneider, R. L. (1998). An alternative to splinting multiple implants: Use of the ITI system. *J Prosthodont,* 7, 114-119.

Vázquez Álvarez, R, Pérez Sayáns, M., Gayoso Diaz, P., & García García, A. (2015). Factors affecting peri-implant bone loss: a post-five-year retrospective study. *Clin Oral Implants Res,* 26, 1006-1014.

Yang, T. C., Maeda, Y., & Gonda, T. (2011). Biomechanical rationale for short implants in splinted restorations: an in vitro study. *Int J Prosthodont,* 24, 130-132.

Torcato, L. B., Pellizzer, E. P., Verri, F. R., Falcón-Antenucci, R. M., Batista, V. E., & Lopes, L. F. (2014). Effect of the parafunctional occlusal loading and crown height on stress distribution. *Braz Dent J*, 25, 554-560.

Verri, F. R., Cruz, R. S., de Souza Batista, V. E., Almeida, D. A., Verri, A. C., Lemos, C. A., Santiago, J. F. Jr., & Pellizzer, E. P. (2016). Can the modeling for simplification of a dental implant surface affect the accuracy of 3D finite element analysis? *Comput Methods Biomech Biomed Engin,* 19, 1665-1672.

Verri, F. R., Santiago, J. F. Jr., Almeida. D. A., de Souza Batista, V. E., Araujo Lemos, C. A., Mello, C. C., & Pellizzer, E. P. (2017). Biomechanical three-dimensional finite element analysis of single implant-supported prostheses in the anterior maxilla, with different surgical techniques and implant types. *Int J Oral Maxillofac Implants*, 32, e191-198.

Lekholom, U, & Zarb, G. A. (1985) Patient selection and preparation. In: Branemark PI, Zarb GA, Albrektsson T, editors. Tissue-integrated prostheses: osseointegration in clinical dentistry. *Chicago: Quintessence*, 199-220.

Puri, N., Pradhan, K. L., Chandna, A., Sehgal, V., & Gupta, R. (2007). Biometric study of tooth size in normal, crowded, and spaced permanent dentitions. *Am J Orthod Dentofacial Orth*op, 132, e7-14.

Nishioka, R. S., de Vasconcellos, L. G., & de Melo Nishioka, G. N. (2011). Comparative strain gauge analysis of external and internal hexagon, Morse taper, and influence of straight and offset implant configuration. *Implant Dent,* 20, e24-32.

Nishioka, R. S., de Vasconcellos, L. G., & de Melo Nishioka, L. N. (2009). External hexagon and internal hexagon in straight and offset implant placement: strain gauge analysis. *Implant Dent,* 18, 512-520.

Sütpideler, M., Eckert, S. E., Zobitz, M., & An, K. N. (2004). Finite element analysis of effect of prosthesis height, angle of force application, and implant offset on supporting bone. *Int J Oral Maxillofac Implants, 19, 819-125.*

Sertgöz A. (1997). Finite element analysis study of the effect of superstructure material on stress distribution in an implant-supported fixed prosthesis. Int J Prosthodont, 10, 19-27.

Sevimay, M., Turhan, F., Kiliçarslan, M. A., & Eskitascioglu, G. (2005). Three-dimensional finite element analysis of the effect of different bone quality on stress distribution in an implant-supported crown. *J Prosthet Dent,* 93, 227-234.

Verri, F. R., Cruz, R. S., Lemos, C. A., de Souza Batista, V. E., Almeida, D. A., Verri, A. C., & Pellizzer, E. P. (2017b). Influence of bicortical techniques in internal connection placed in premaxillary area by 3D finite element analysis. *Comput Methods Biomech Biomed Engin*, 20, 193-200.

Pellizzer, E. P., Lemos, C. A. A., Almeida, D. A. F., de Souza Batista, V. E., Santiago Júnior, J. F., & Verri, F. R. (2018). Biomechanical analysis of different implant-abutments interfaces in different bone types: An in silico analysis. *Mater Sci Eng C Mater Biol Appl,* 90, 645-650.

de Souza Batista, V. E., Verri, F. R., Almeida, D. A., Santiago, J. F. Jr., Lemos, C. A., & Pellizzer, E. P. (2017b). Finite element analysis of implant-supported prosthesis with pontic and cantilever in the posterior maxilla. *Comput Methods Biomech Biomed Engin,* 20, 663-670.

Frost, H. M. (2003). Bone's mechanostat: A 2003 update. *Anat Rec A Discov Mol Cell Evol Biol*, 275, 1081-1101.

Mendonça, J. A., Francischone, C. E., Senna, P. M., Matos de Oliveira, A. E., & Sotto-Maior, B. S. (2014). A retrospective evaluation of the survival rates of splinted and non-splinted short dental implants in posterior partially edentulous jaws. *J Periodontol,* 85, 787-794.

Baggi, L., Cappelloni, I., Di Girolamo, M., Maceri, F., & Vairo, G. (2008). The influence of implant diameter and length on stress distribution of osseointegrated implants related to crestal bone geometry: a three-dimensional finite element analysis. *J Prosthet Dent,* 100, 422-431.

Ueda, N., Takayama, Y., & Yokoyama, A. (2017). Minimization of dental implant diameter and length according to bone quality determined by finite element analysis and optimized calculation. *J Prosthodont Res.* 61, 324-332.

Goiato, M. C., Pellizzer, E. P., da Silva, E. V., Bonatto, L. R., & dos Santos, D. M. (2015). Is the internal connection more efficient than external connection in mechanical, biological, and esthetical point of views? A systematic review. *Oral Maxillofac Surg,* 19, 229-242.

Minatel, L., Verri, F. R., Kudo, G. A. H., de Faria Almeida, D. A., de Souza Batista, V. E., Lemos, C. A. A., Pellizzer, E. P., & Santiago Jr., J. F. (2017). Effect of different types of prosthetic platforms on stress-distribution in dental implant-supported prostheses. *Mater Sci Eng C Mater Biol Appl,* 71, 35-42.

Itoh, H., Caputo, A. A., Kuroe, T., & Nakahara, H. (2004). Biomechanical comparison of straight and staggered implant placement configurations. *Int J Periodontics Restorative Dent*, 24, 47-55.